National Astronomical Observatories
Chinese Academy of Sciences

Recovering lost 21 cm radial modes with tidal reconstruction

Hong-Ming Zhu 朱弘明

National Astronomical Observatories, CAS

21 cm Cosmology Workshop 2024, Hangzhou 2024

21 cm radial modes

- HI foregrounds: smooth
- Contaminates low k radial density modes
- No cross correlation!

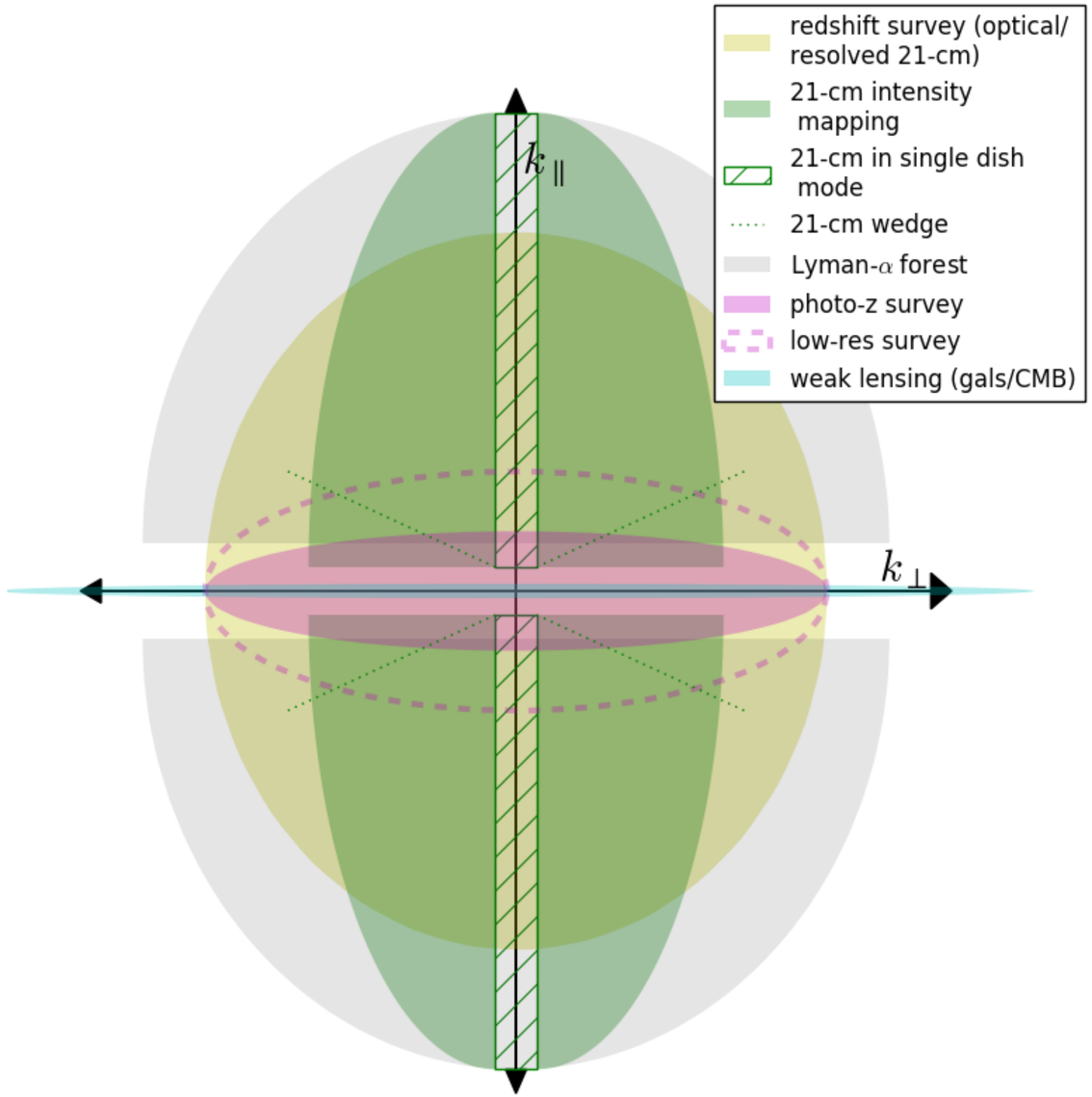

Credit: A. Slosar

Mpc scale HI detection

- MeerKAT auto P(k)
- Foreground avoidance
- Mpc probe of HI halo
- Cosmological probe?

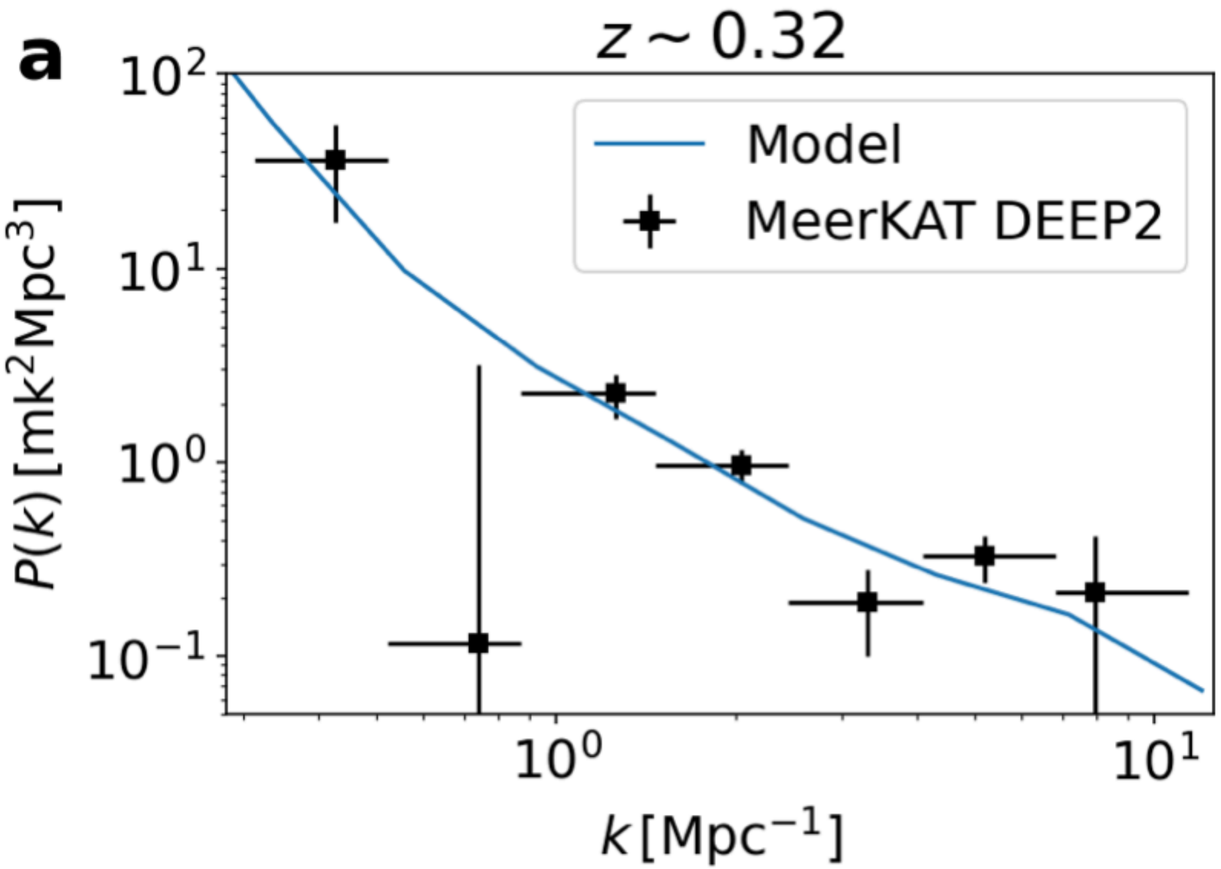

Paul et al, 2023

Power spectrum covariance

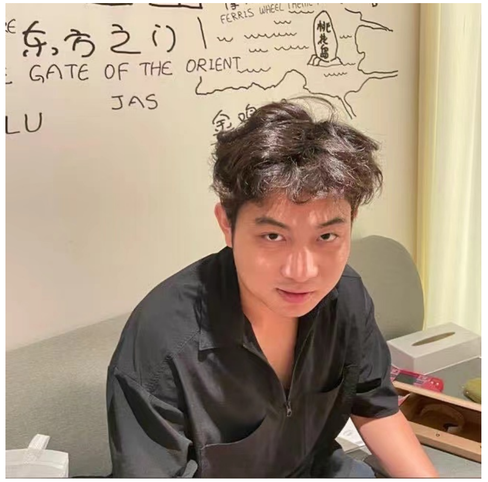

UGS at THU -> GS at Madison

- Power spectrum: $P_i = P(k_i)$
- Covariance matrix: $\hat{C}_{ij} = \langle (P_i - \langle P_i \rangle)(P_j - \langle P_j \rangle) \rangle$
- Linear initial conditions (a Gaussian random field): $C_{ij} = \frac{2[P(k_i)]^2}{N_{k_i}} \delta_{ij}$
- Nonlinear evolution generate off-diagonal measurements:

$$C_{ij} \neq 0$$

Zang & **Zhu***, **ApJ** 961, 160, 2024

Power spectrum covariance

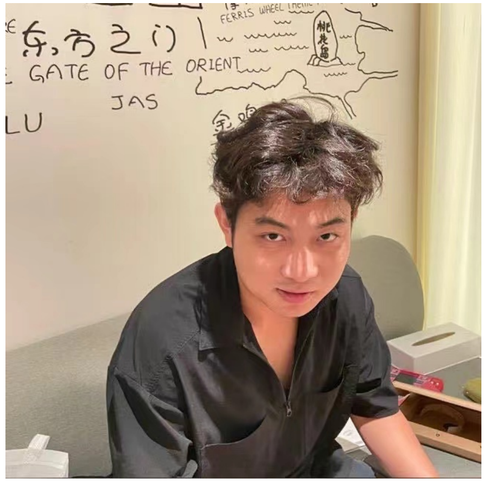

UGS at THU -> GS at Madison

- Power spectrum: $P_i = P(k_i)$
- Covariance matrix: $\hat{C}_{ij} = \langle (P_i - \langle P_i \rangle)(P_j - \langle P_j \rangle) \rangle$

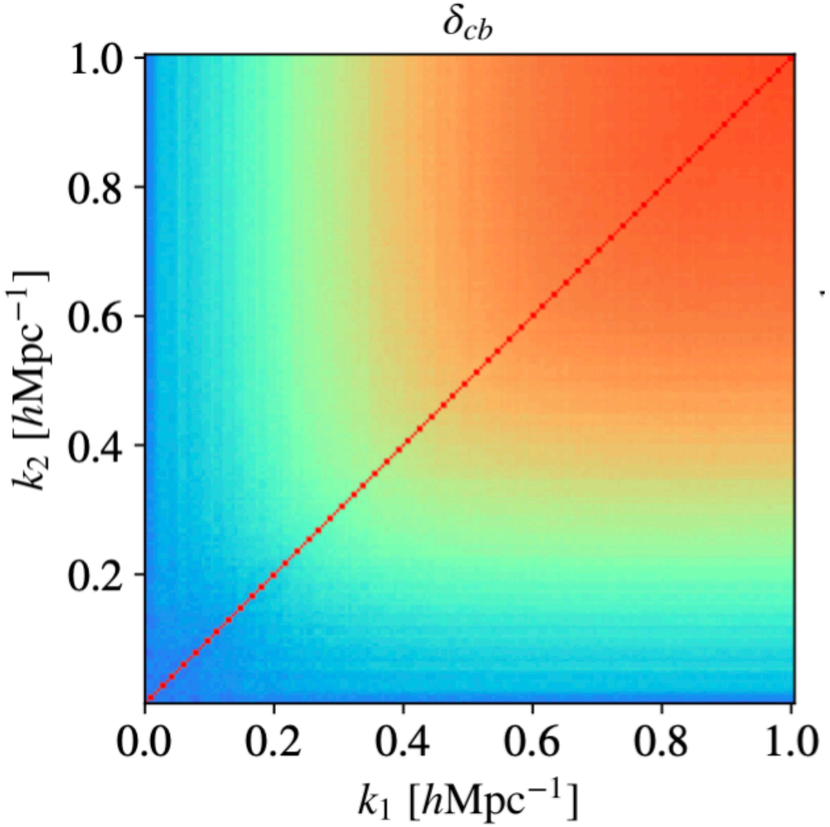

Strong non-diagonal correlation in power spectrum covariance!

Zang & **Zhu***, **ApJ** 961, 160, 2024

Fisher information

- Fisher matrix: $F_{\alpha\beta} = \sum_{i,j} \frac{\partial P_i}{\partial \theta_\alpha} C_{ij}^{-1} \frac{\partial P_j}{\partial \theta_\beta}$ $\sigma(\theta_\alpha) = \sqrt{(F^{-1})_{\alpha\alpha}}$

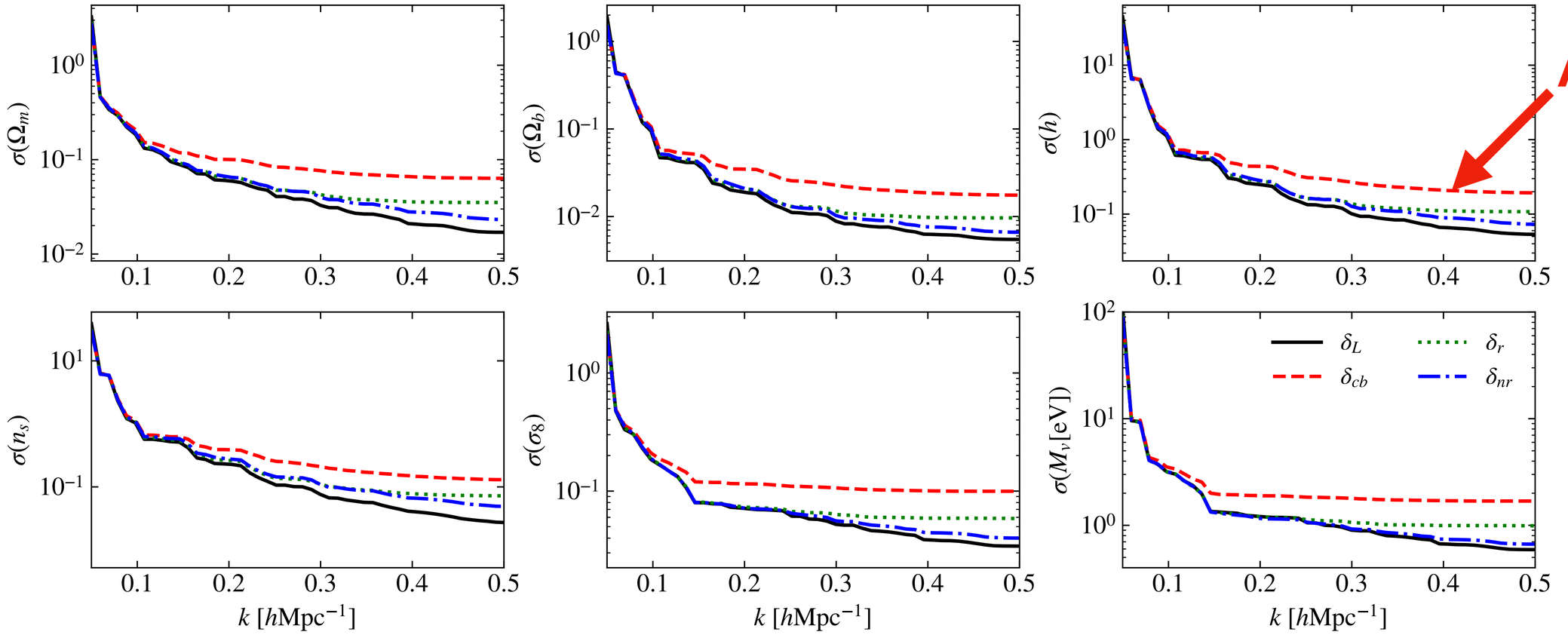

A plateau!

Zang & **Zhu***, **ApJ** 961, 160, 2024

How to extract from NL scales?

Need to go from NL to Linear scales

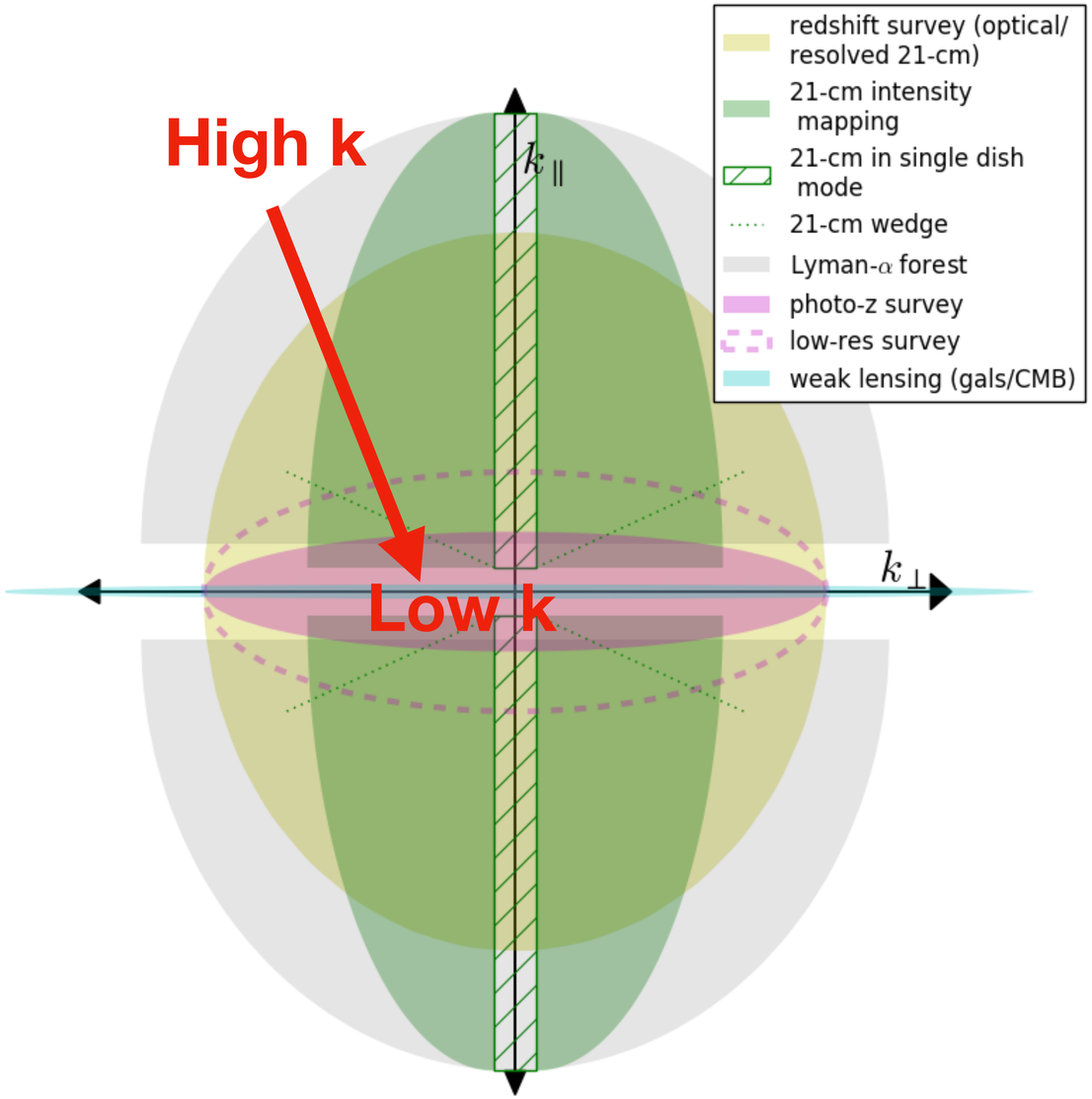

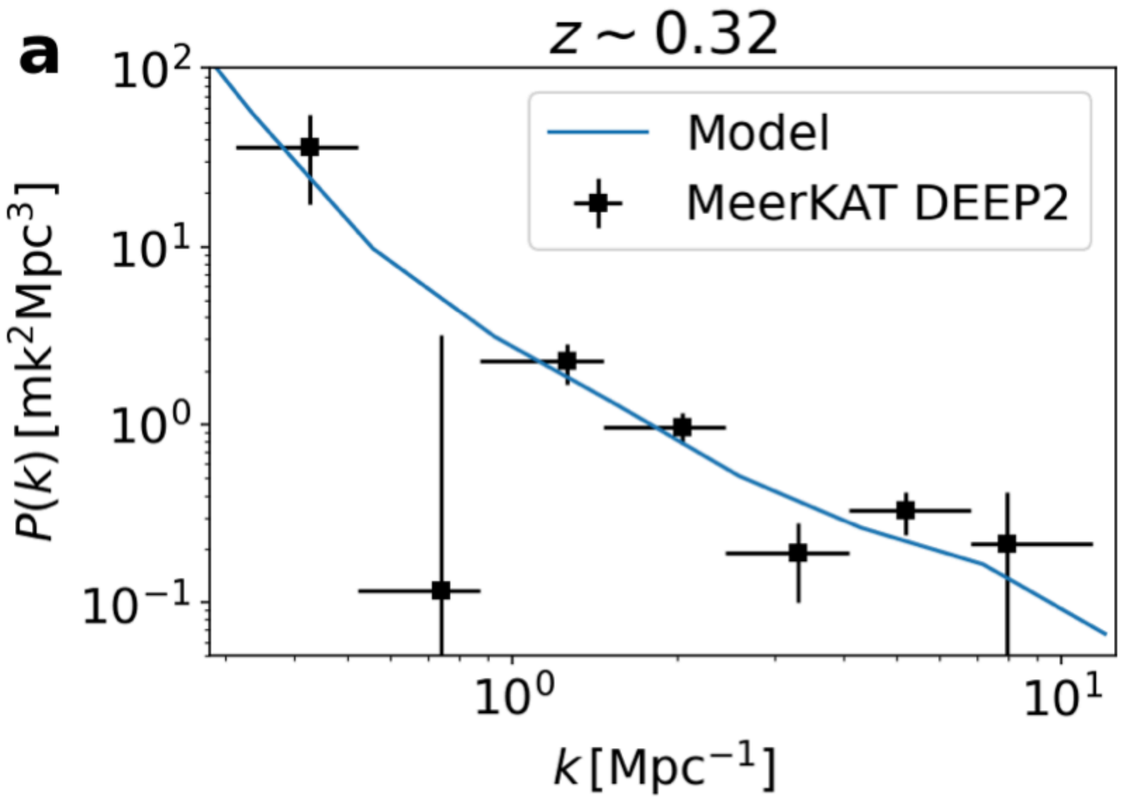

Credit: A. Slosar

Paul et al, 2023

Cosmic web: gravitational coupling

- Cosmic tides from residual anisotropic gravity forces

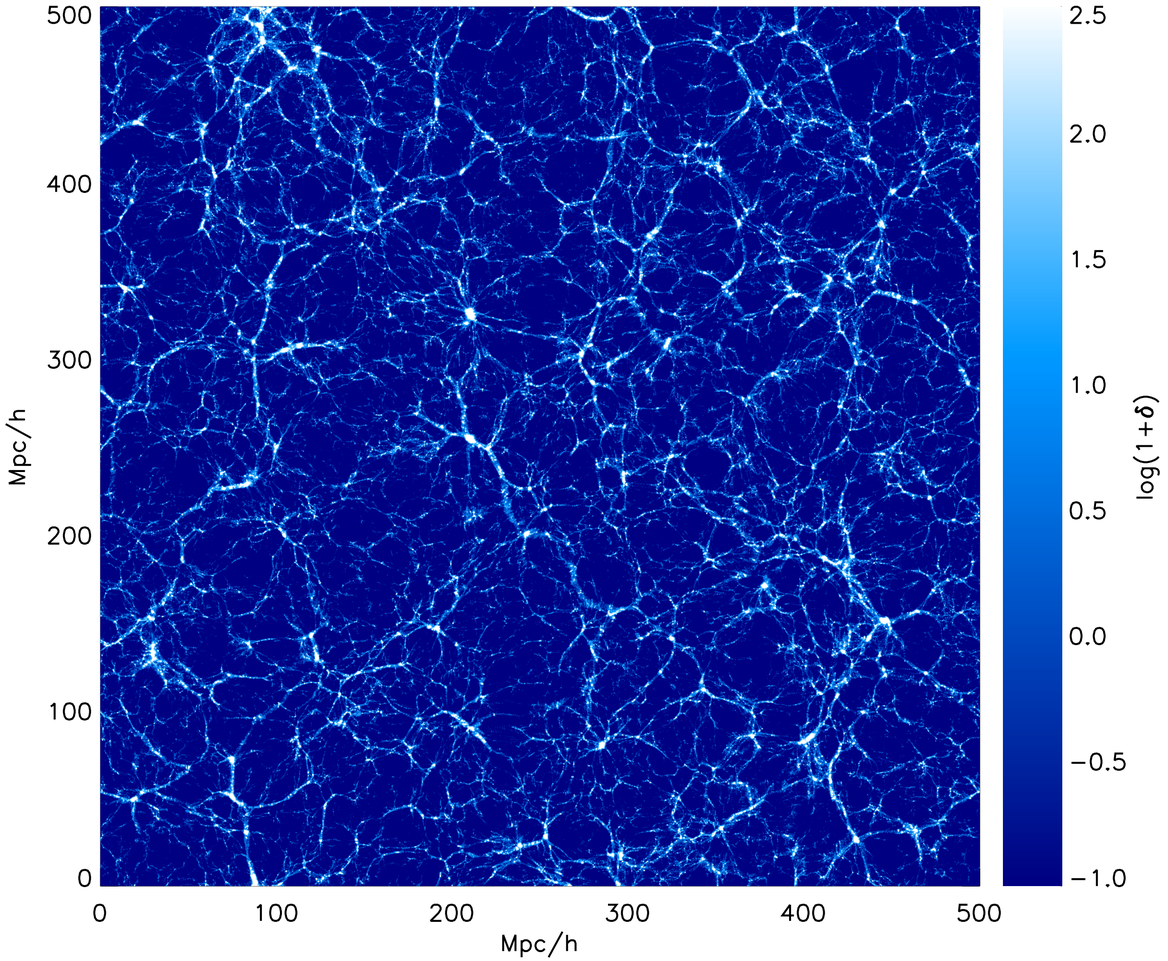

Pen, Zhu, Chen, Foreman, Li, Dodelson, Croft, Wang, Jeong, Sherwin, Moodley, Guandalin, Gagnon-Hartman, Modi, White, Slosar, ++

Tidal reconstruction vs weak lensing

- Cosmic tides and weak lensing

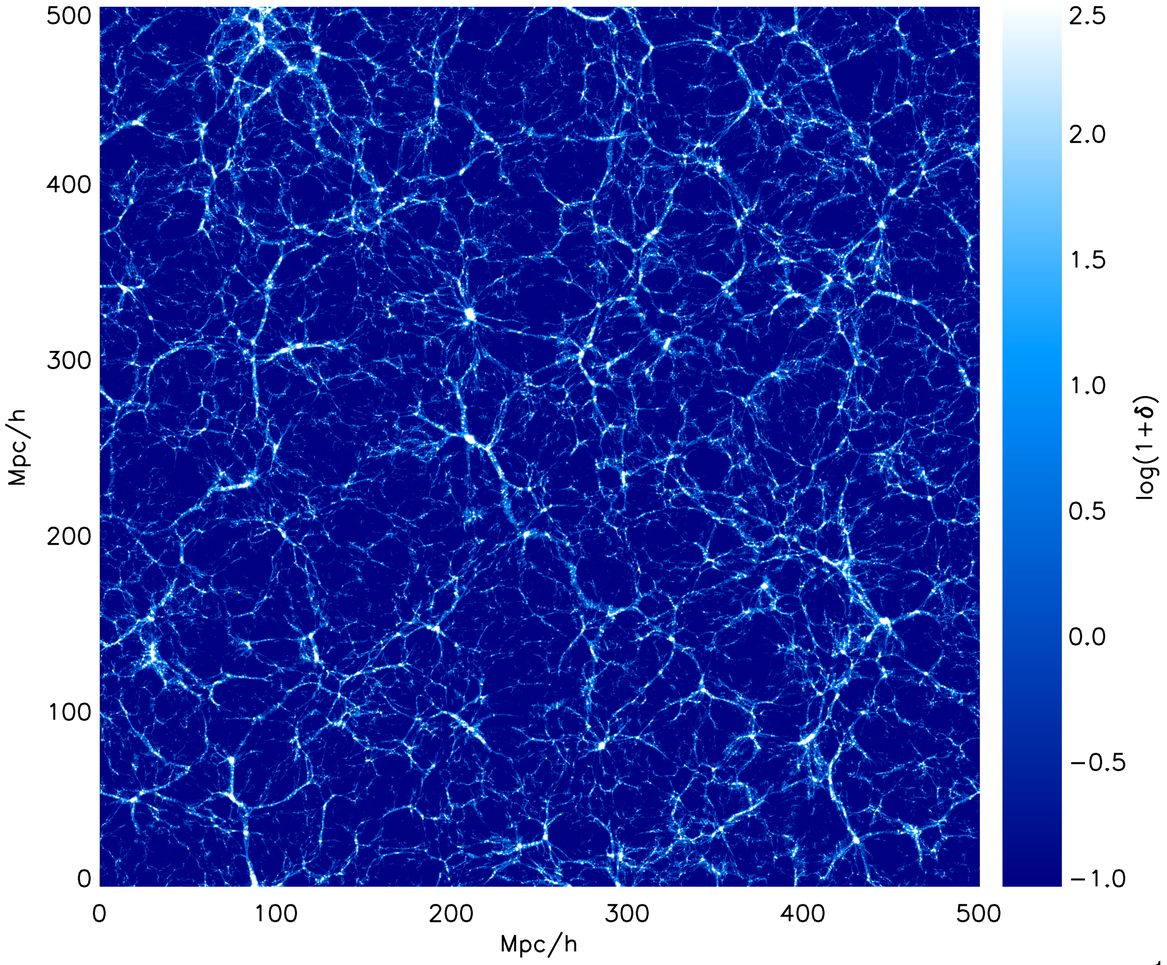

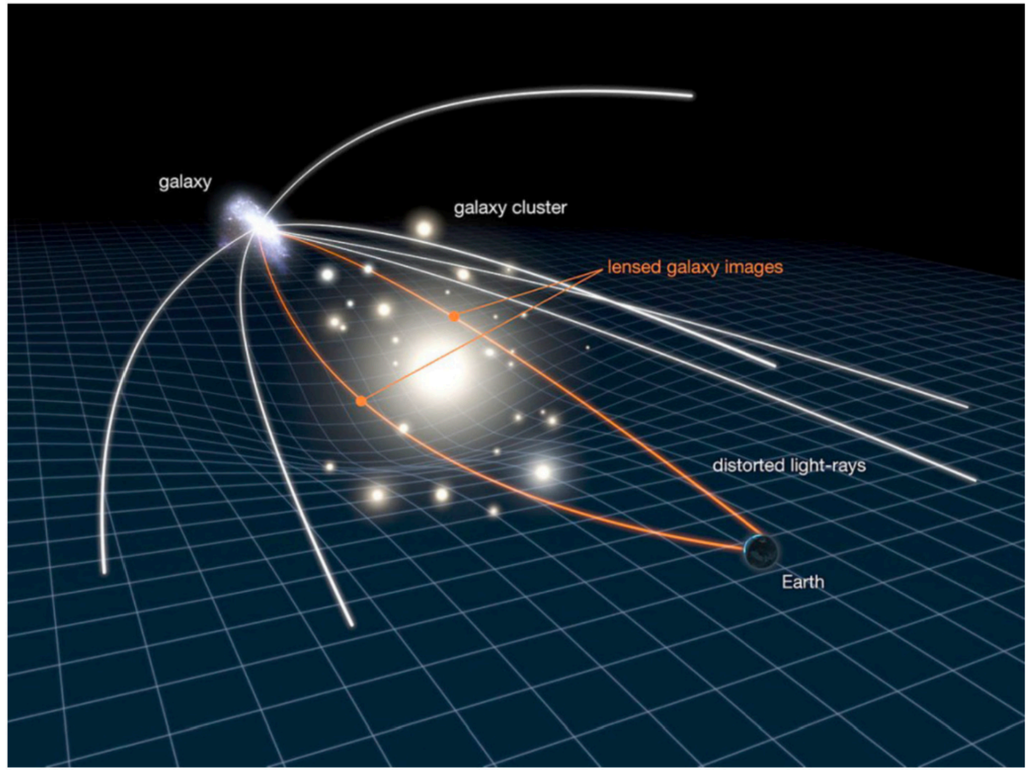

FIGURE 3.4 Sketch illustrating how the curvature of spacetime induced by a massive cluster of galaxies deflects the trajectories of passing light rays. The same curvature also keeps the galaxies in orbit within the cluster. Both effects are described by Eq. (3.72). From www.cfhtlens.org.

Dodelson & Schmidt, Modern Cosmology (2020)

Tidal reconstruction vs weak lensing

- Lensing deflection: $\boldsymbol{\theta}_S = \boldsymbol{\theta} + \boldsymbol{\alpha}$
- Convergence and shear: $\dfrac{\partial \theta_i^S}{\partial \theta_j} = \begin{pmatrix} 1-\kappa-\gamma_1 & -\gamma_2 \\ -\gamma_2 & 1-\kappa+\gamma_1 \end{pmatrix}$

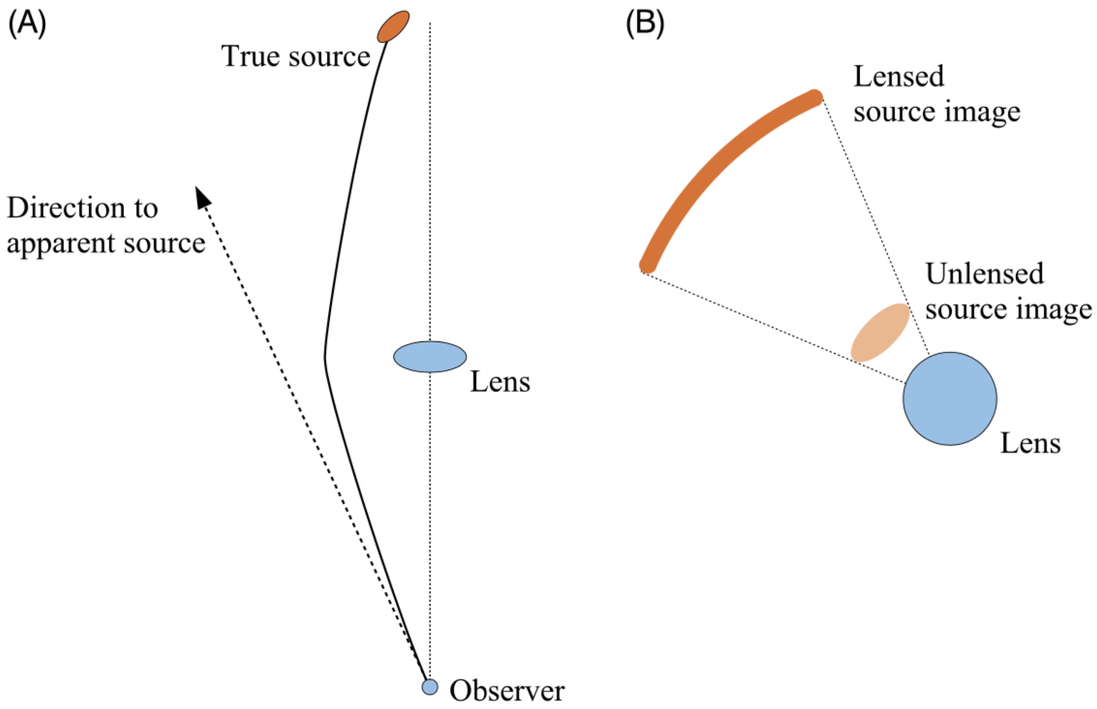

Dodelson & Schmidt, Modern Cosmology (2020)

Tidal reconstruction vs weak lensing

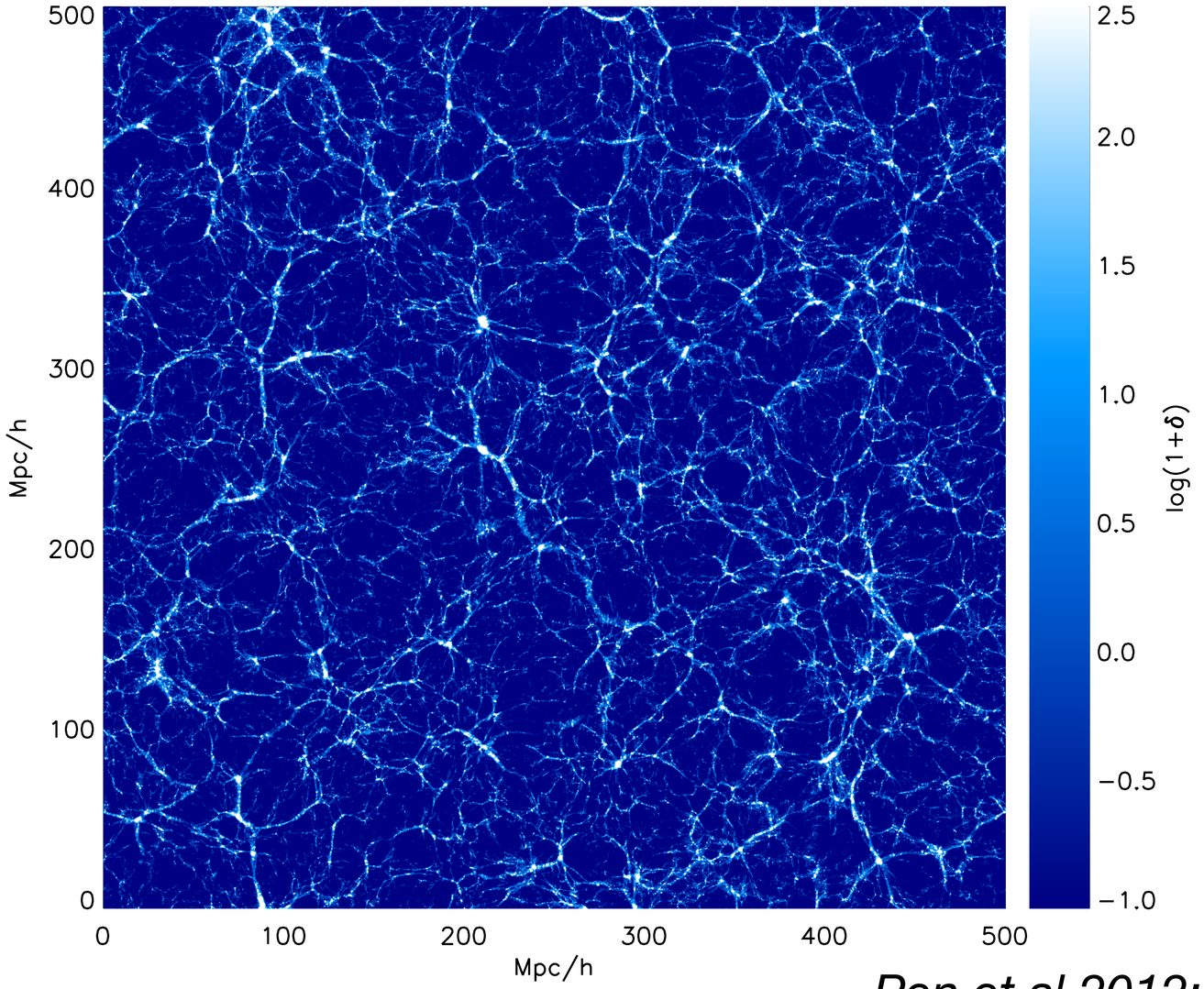

- Tidal field: $t_{ij} = \Phi_{L,ij}$
- Decomposition:

$$t_{ij} = \begin{pmatrix} \epsilon_0 + \epsilon_1 - \epsilon_z & \epsilon_2 & \epsilon_x \\ \epsilon_2 & \epsilon_0 - \epsilon_1 - \epsilon_z & \epsilon_y \\ \epsilon_x & \epsilon_y & \epsilon_0 + 2\epsilon_z \end{pmatrix}$$

- Analogy with CMB lensing

$$\begin{aligned}
\hat{\epsilon}_1(\boldsymbol{x}) &= [\delta^{w_1}(\boldsymbol{x})\delta^{w_1}(\boldsymbol{x}) - \delta^{w_2}(\boldsymbol{x})\delta^{w_2}(\boldsymbol{x})]/2, \\
\hat{\epsilon}_2(\boldsymbol{x}) &= \delta^{w_1}(\boldsymbol{x})\delta^{w_2}(\boldsymbol{x}), \\
\hat{\epsilon}_x(\boldsymbol{x}) &= \delta^{w_1}(\boldsymbol{x})\delta^{w_3}(\boldsymbol{x}), \\
\hat{\epsilon}_y(\boldsymbol{x}) &= \delta^{w_2}(\boldsymbol{x})\delta^{w_3}(\boldsymbol{x}), \\
\hat{\epsilon}_z(\boldsymbol{x}) &= [2\delta^{w_3}(\boldsymbol{x})\delta^{w_3}(\boldsymbol{x}) - \delta^{w_1}(\boldsymbol{x})\delta^{w_1}(\boldsymbol{x}) \\
&\quad - \delta^{w_2}(\boldsymbol{x})\delta^{w_2}(\boldsymbol{x})]/6,
\end{aligned}$$

where

$$\delta^{w_j}(\boldsymbol{k}) = i\hat{k}_j w(k)\delta(\boldsymbol{k})N^{1/2}_{\epsilon_\alpha},$$

*Pen et al 2012; **Zhu** et al 2016, 2018, 2022; Zang, **Zhu*** et al 2024*

Tidal reconstruction: Halos

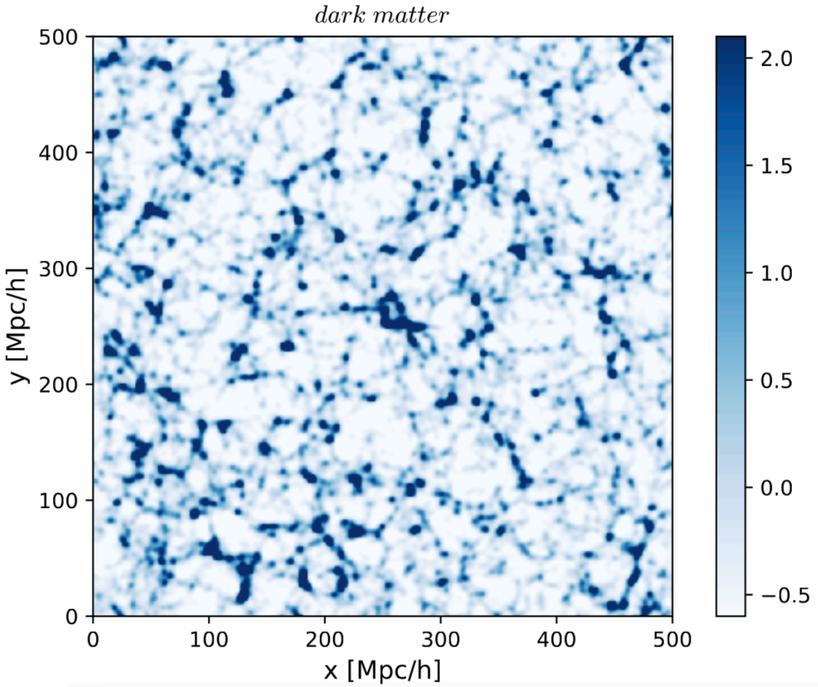

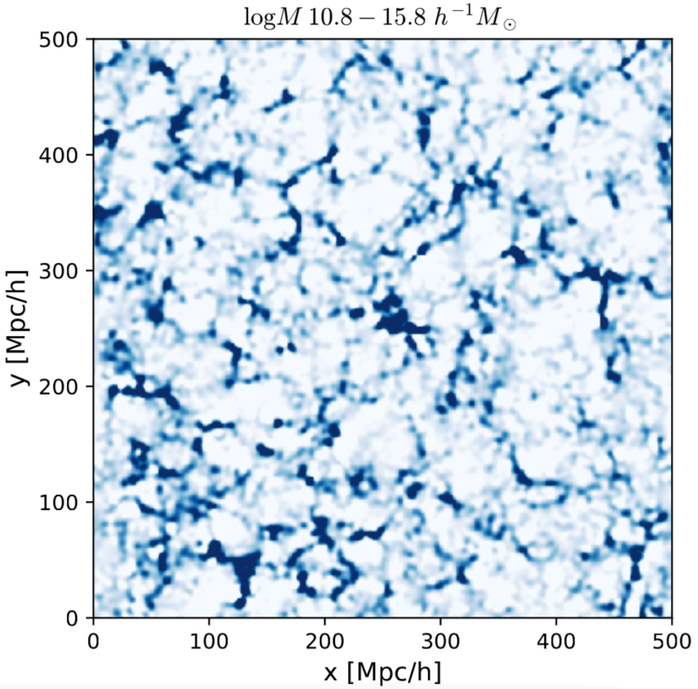

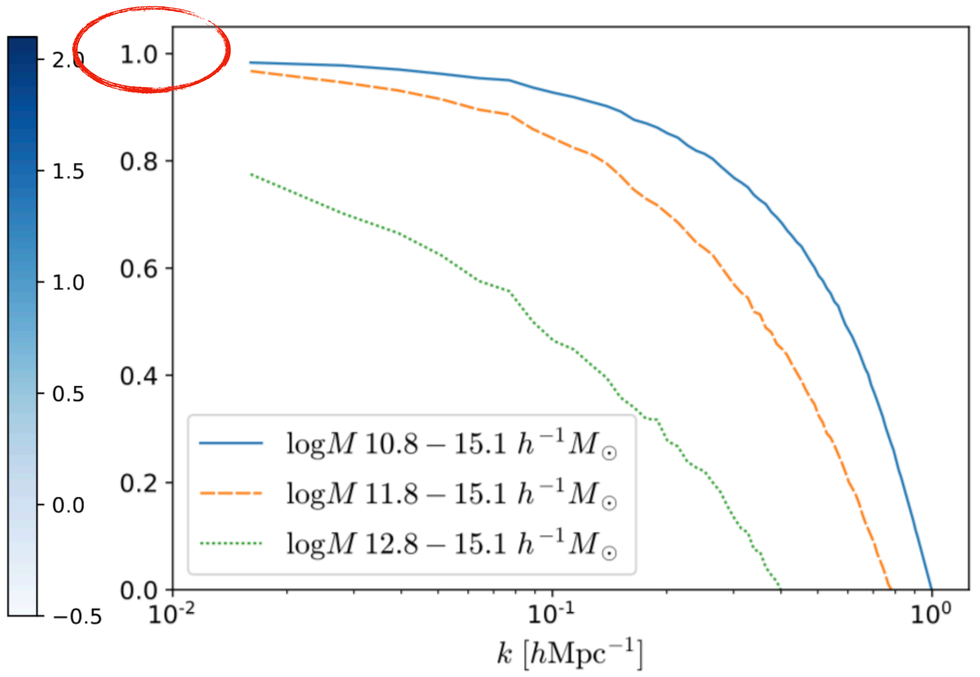

DM field

Reconstructed

$$r(k) = \frac{P_{\delta_r \delta}(k)}{\sqrt{P_{\delta_r \delta_r}(k) P_{\delta\delta}(k)}}$$

***Zhu** et al, 2022*

Tidal reconstruction: redshift space

- Redshift space halo fields:

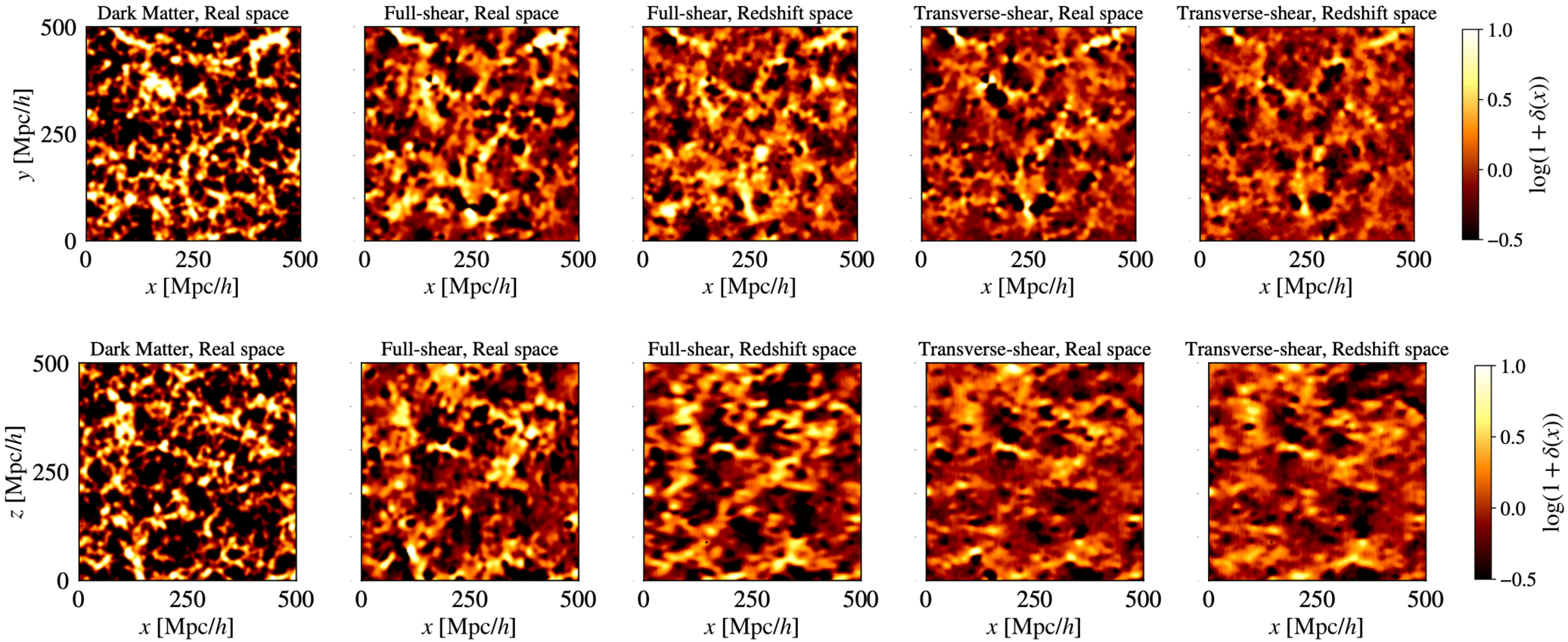

*Zang, **Zhu*** et al 2024*

Applications: 21 cm radial modes

Before reconstruction

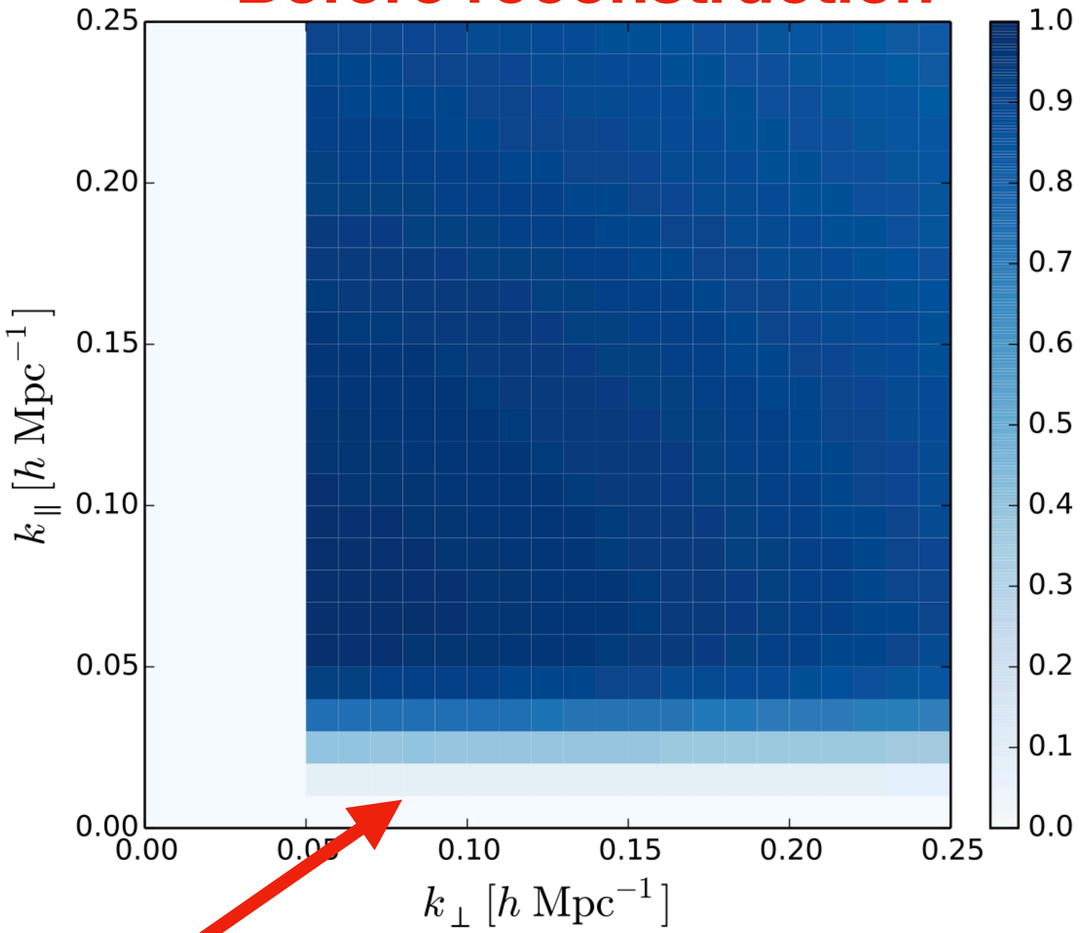

Foreground

Tidal reconstruction

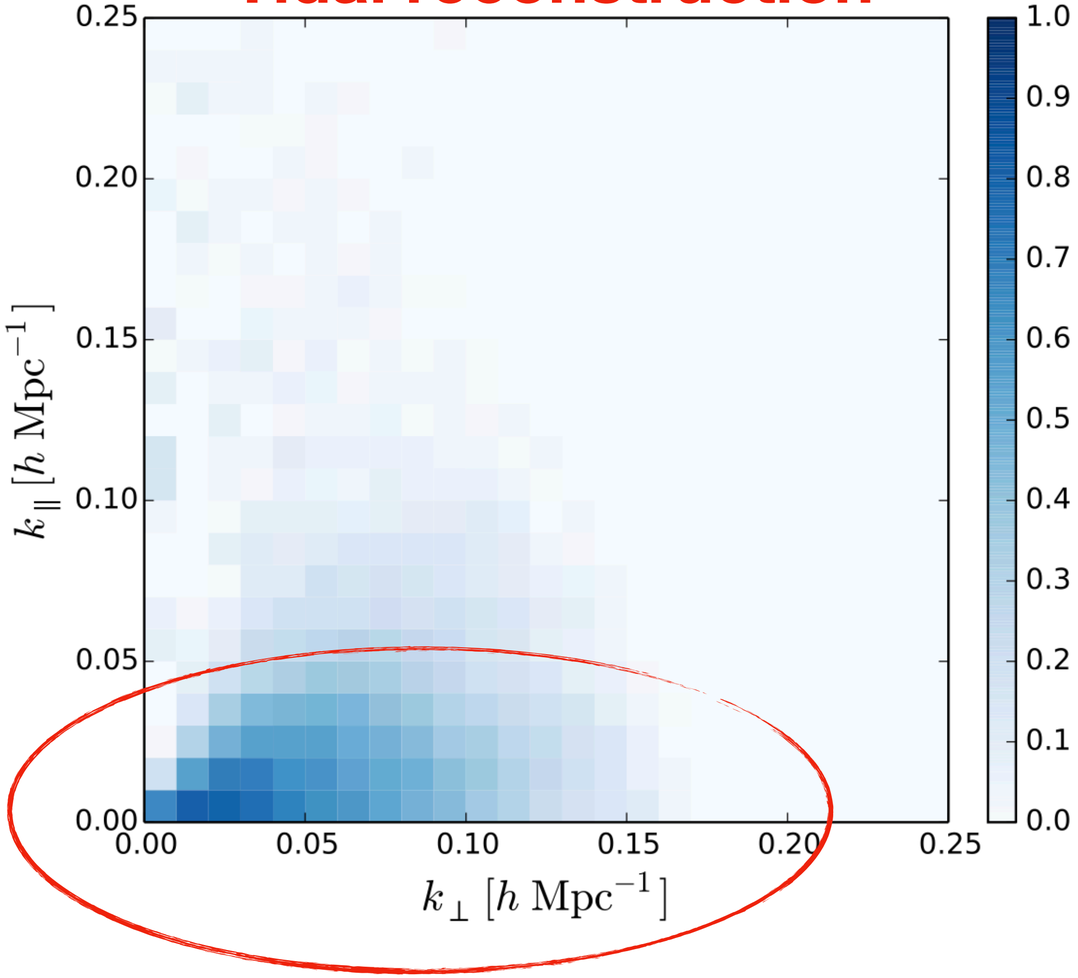

Zhu et al. **PRD** 98, 043511 (2018)

Applications: 21 cm-lensing

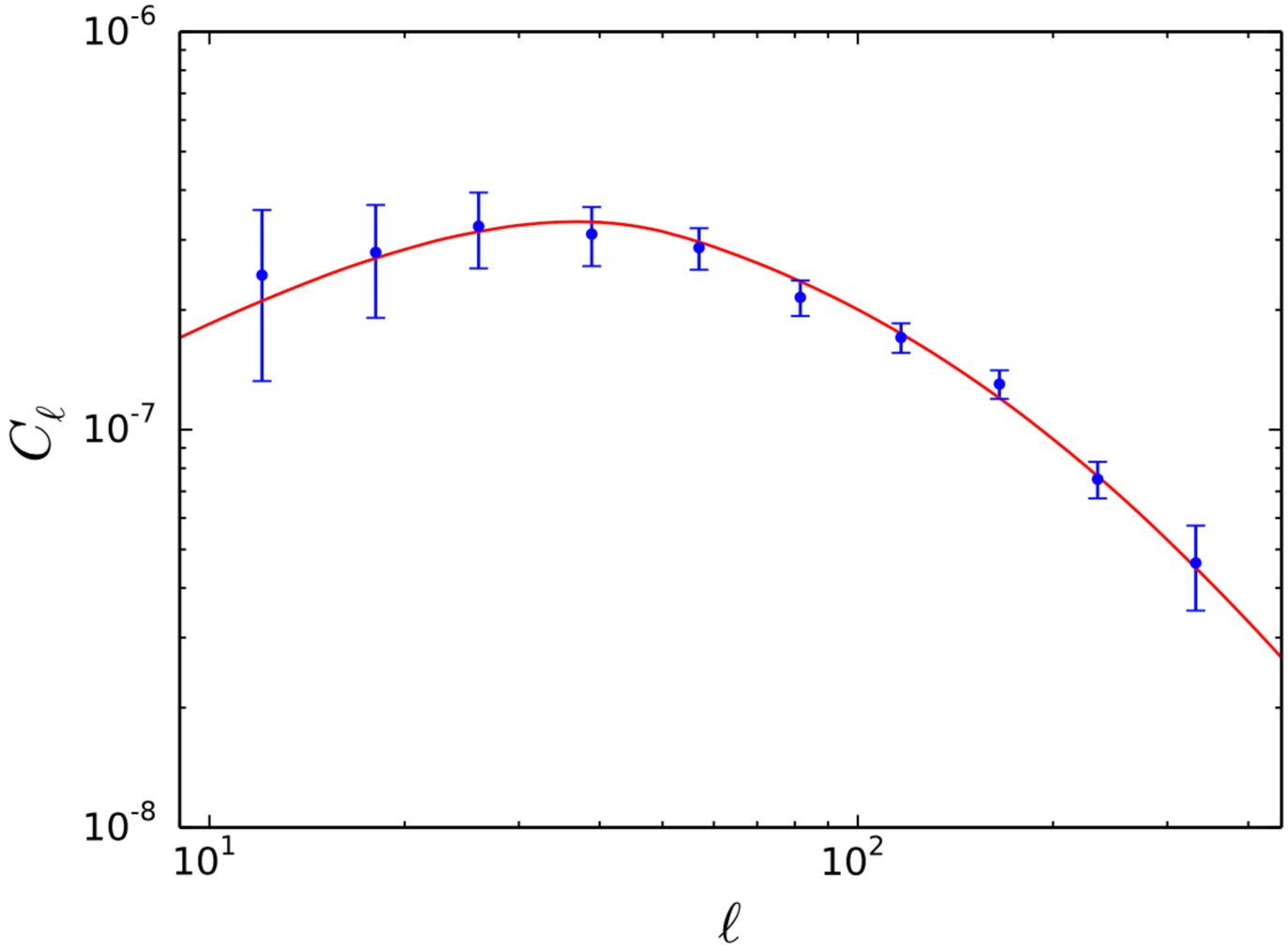

Zhu et al. **PRD** 98, 043511 (2018)

Applications: 21 cm-ISW

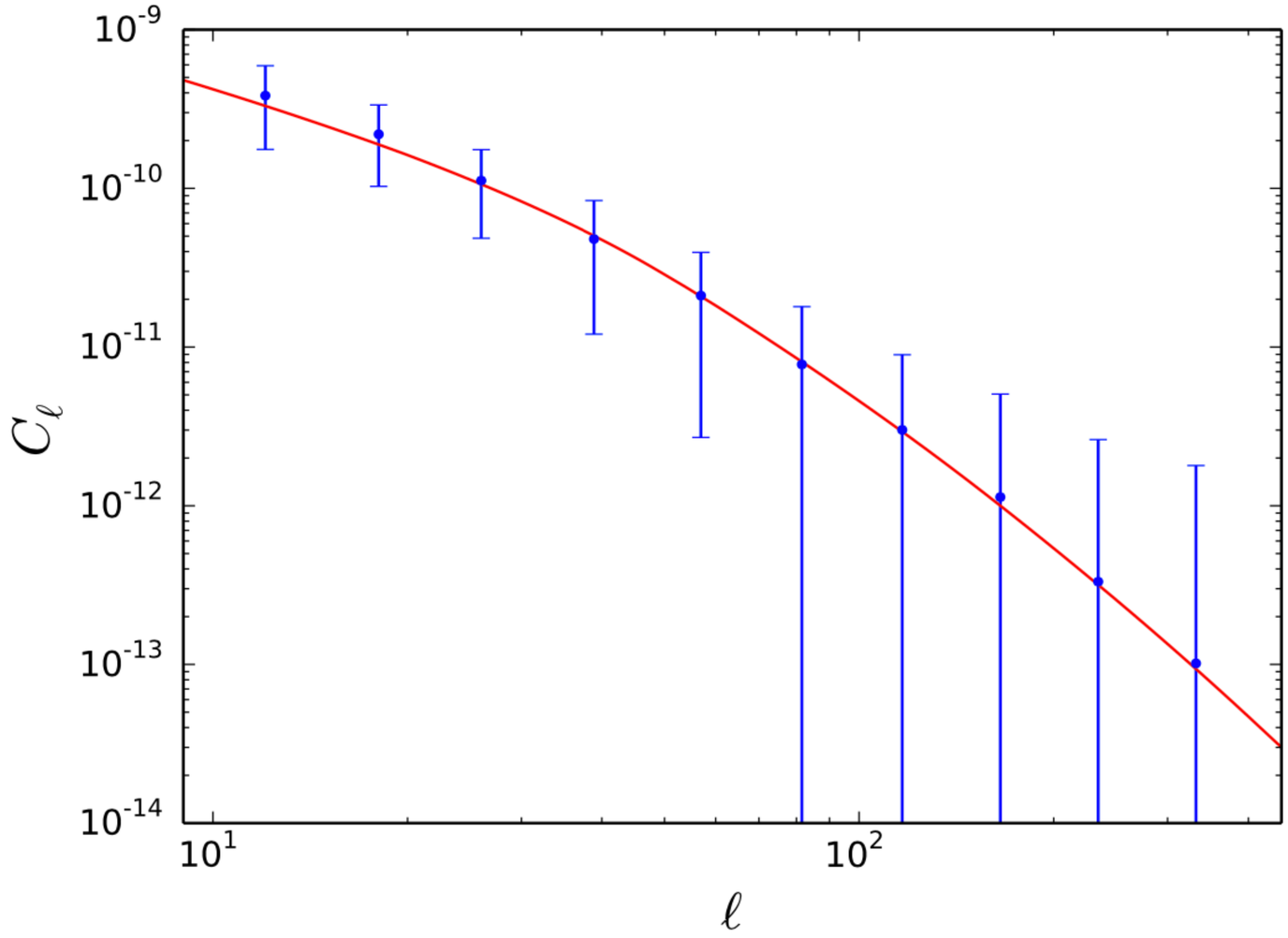

Zhu et al. **PRD** 98, 043511 (2018)

Applications: 21 cm-photo-z

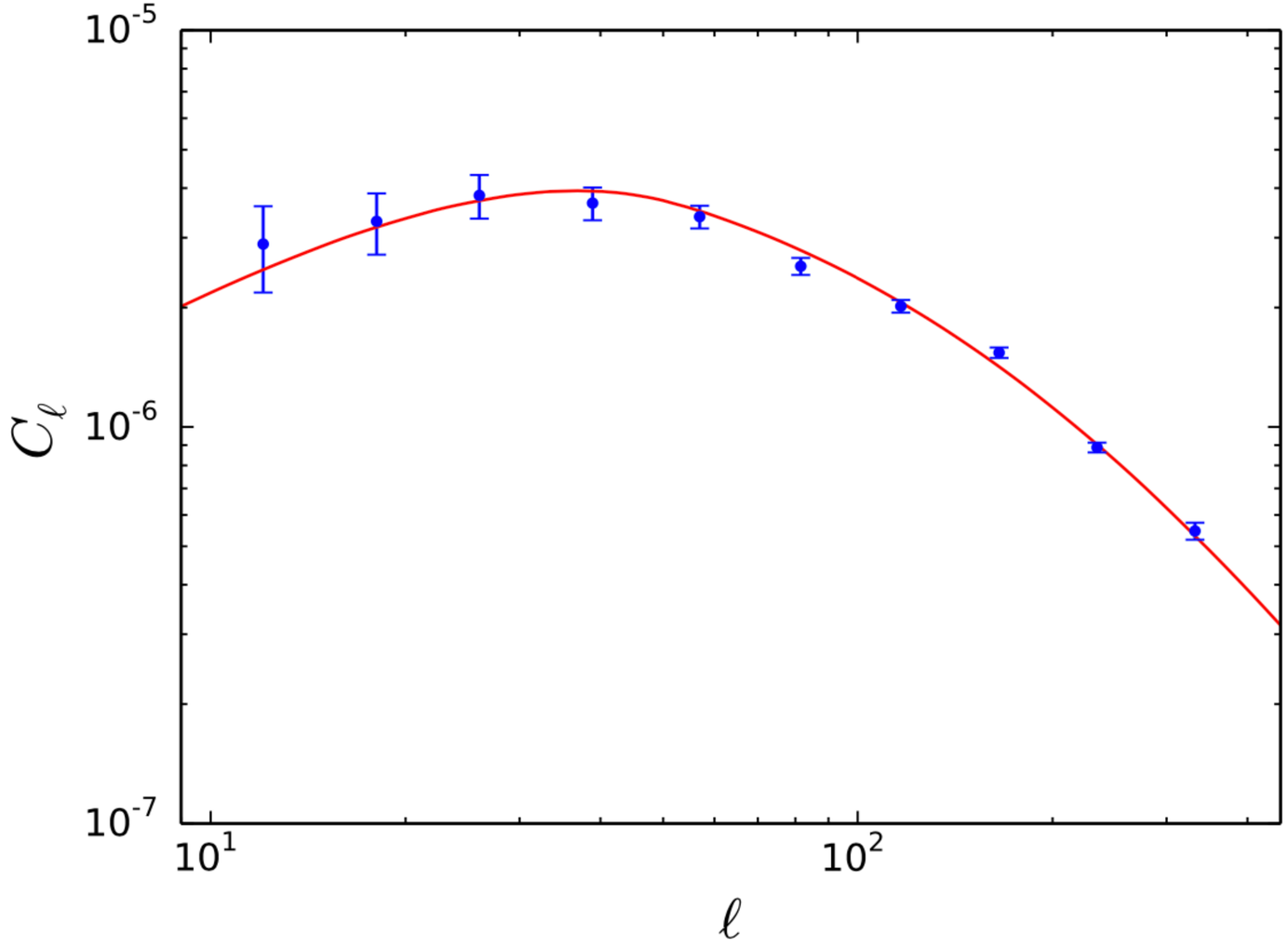

Zhu et al. **PRD** 98, 043511 (2018)

Cosmic tidal reconstruction

Cosmic Visions Dark Energy:
Inflation and Early Dark Energy with a Stage II
Hydrogen Intensity Mapping Experiment
(Cosmic Visions 21 cm Collaboration)

Réza Ansari,[1] Evan J. Arena,[2,3] Kevin Bandura,[4,5] Philip Bull,[6,7] Emanuele Castorina,[8] Tzu-Ching Chang,[9,10] Shi-Fan Chen,[8] Liam Connor,[11] Simon Foreman,[12] Josef Frisch,[13] Daniel Green,[14] Matthew C. Johnson,[15,16] Dionysios Karagiannis,[17] Adrian Liu,[6,7,18] Kiyoshi W. Masui,[19] P. Daniel Meerburg,[20,21,22,23,24] Moritz Münchmeyer,[16] Laura B. Newburgh,[25] Andrej Obuljen,[26,27,28] Paul O'Connor,[2] Hamsa Padmanabhan,[12] J. Richard Shaw,[29] Chris Sheehy,[2] Anže Slosar,[2,*] Kendrick Smith,[16] Paul Stankus,[30] Albert Stebbins,[31] Peter Timbie,[32] Francisco Villaescusa-Navarro,[33] Benjamin Wallisch,[14,34] and Martin White[6]

)rsay, France

Cosmic Visions 21 cm collaboration white paper, 2.8. Weak lensing and tidal reconstruction) 。

Cosmic tidal reconstruction

Snowmass 2021

Improving signal recovery. Significant numbers of modes are lost to foregrounds, which reduces our constraining ability generally, but particularly affects science that needs access to the largest scales. Improved foreground removal that reduces the effect of the wedge could improve this, as would methods like tidal reconstruction [128–130], but these techniques need substantial development. Similarly, traditional reconstruction techniques [131, 132] that recover non-linear modes need work adapting them for the peculiarities of 21 cm intensity mapping.

Vector and tensor perturbations

- Metric and matter content

$$g_{00}(t,\boldsymbol{x}) = -1 + h_{00}(t,\boldsymbol{x}),$$
$$g_{0i}(t,\boldsymbol{x}) = a(t)h_{0i}(t,\boldsymbol{x}) = a(t)h_{i0}(t,\boldsymbol{x}),$$
$$g_{ij}(t,\boldsymbol{x}) = a^2(t)\left[\delta_{ij} + h_{ij}(t,\boldsymbol{x})\right],$$

$$h_{00} = -2\Psi,$$
$$h_{0i} = 0,$$
$$h_{ij} = 2\Phi\delta_{ij},$$

$$h_{ij} = 2D\delta_{ij} + 2k_ik_jE + ik_iV_j + ik_jV_i + h_{ij}^{\mathrm{TT}}$$

- Fossil effect: Masui & Pen 2012, Dai++ 2013, Schmidt++ 2014

$$P(k_a) = \tilde{P}(k) - \frac{k_ik_jh^{ij}}{2k}\frac{d\tilde{P}}{dk} + O(\frac{k_h}{k}h_{ij}) + O({h_{ij}}^2)$$

Zhu and Pen, in prep, 2024

Helical vector and tensor perturbations

$$v_a(\boldsymbol{K}) = v_R(\boldsymbol{K}) e_a^R(\hat{\boldsymbol{K}}) + v_L(\boldsymbol{K}) e_a^L(\hat{\boldsymbol{K}})$$

$$h_{ab}(\boldsymbol{K}) = h_R(\boldsymbol{K}) e_{ab}^R(\hat{\boldsymbol{K}}) + h_L(\boldsymbol{K}) e_{ab}^L(\hat{\boldsymbol{K}})$$

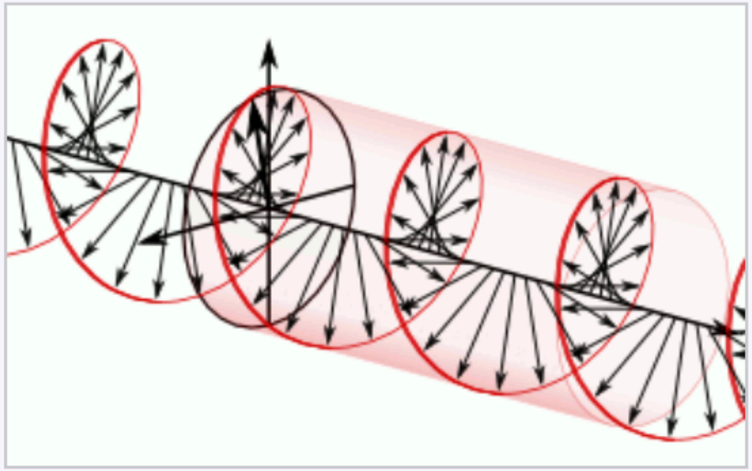

Animation of right-handed (clockwise) circularly polarized light, as defined from the point of view of a receiver in agreement with optics conventions.

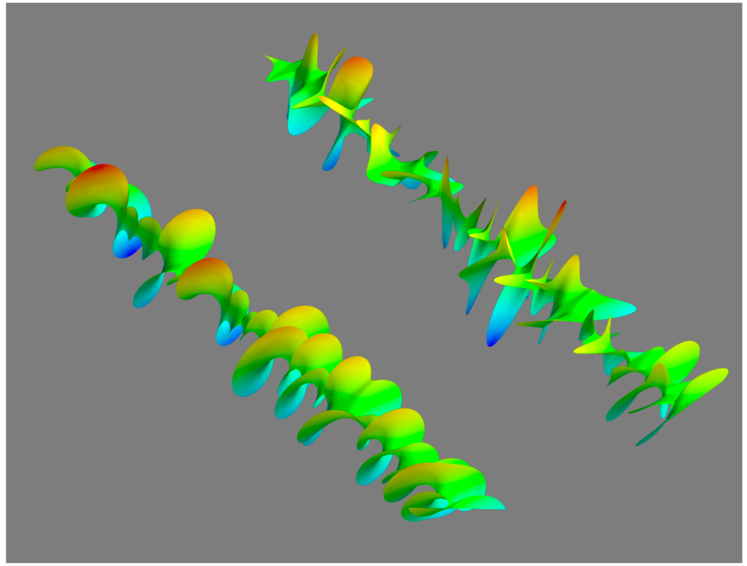

FIG. 1. Visualization of gravity-wave helicity. Shown is the instantaneous strain for two pseudo-1D tensor fields with strain in the $x-y$ plane and wave numbers aligned with the z axis. The width and orientation of the ribbons correspond to magnitude and orientation of the strain. The two fields are generated from the same realization of random numbers but the lower field has all power in the right-hand circular polarization ($\Delta\chi = 1$), whereas the power in the upper field is distributed equally between left- and right-hand circular polarizations ($\Delta\chi = 0$). The realization is drawn from a band-limited white power spectrum.

Image from Wiki

Masui, Pen, Turok, PRL 2017

Helical gravity wave fossils ~ 10%

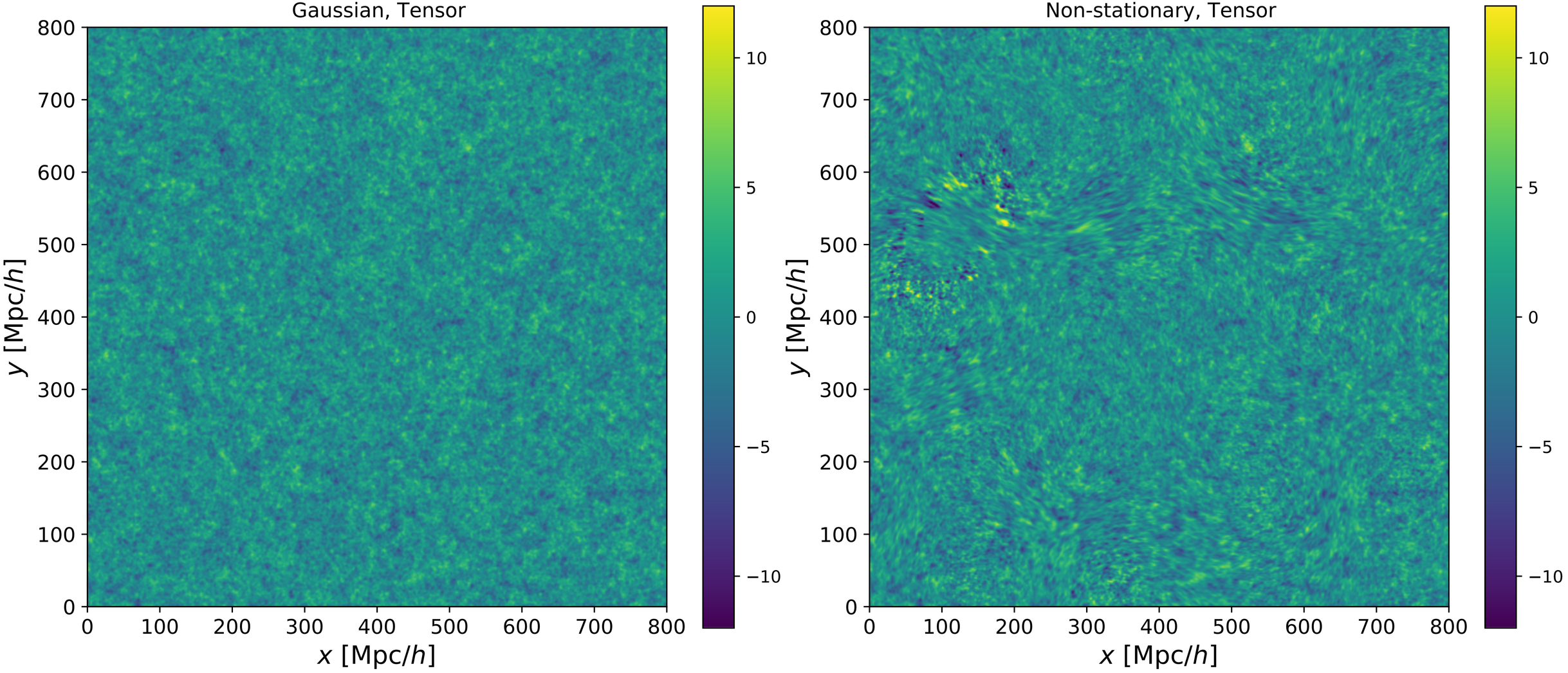

***Zhu** and Pen, in prep, 2024*

Helical gravity wave fossils

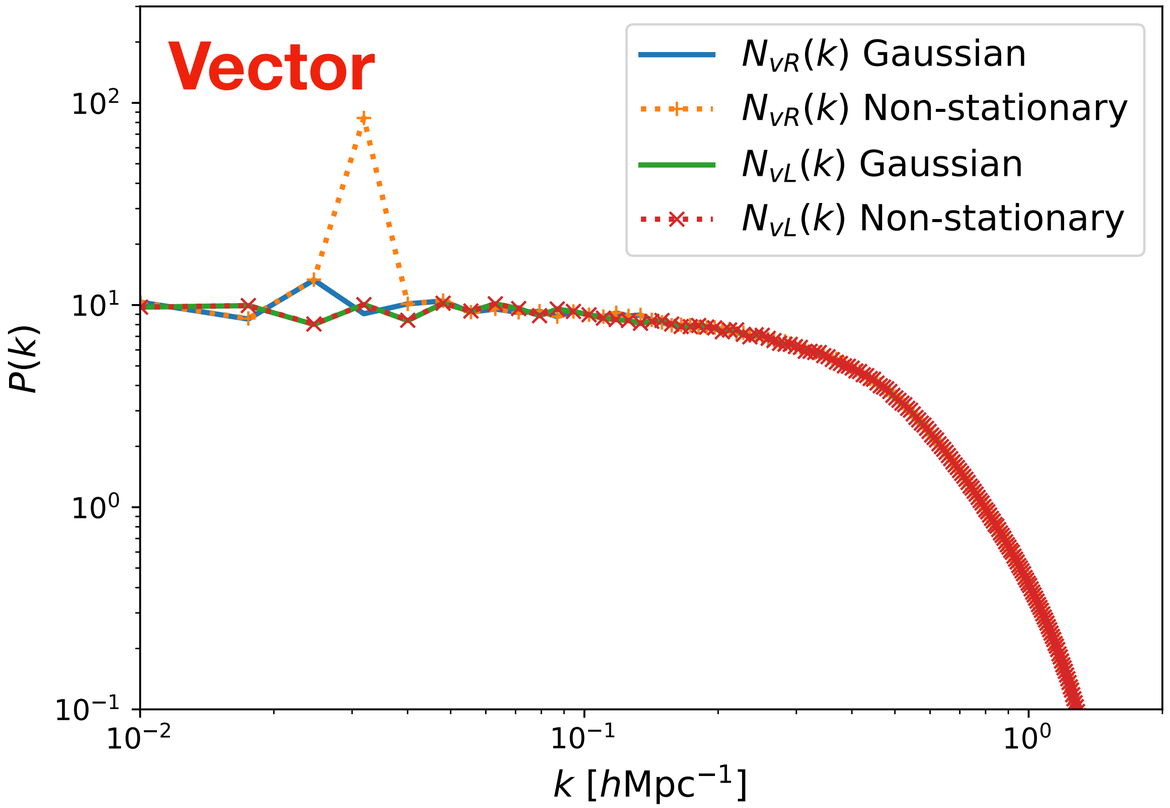

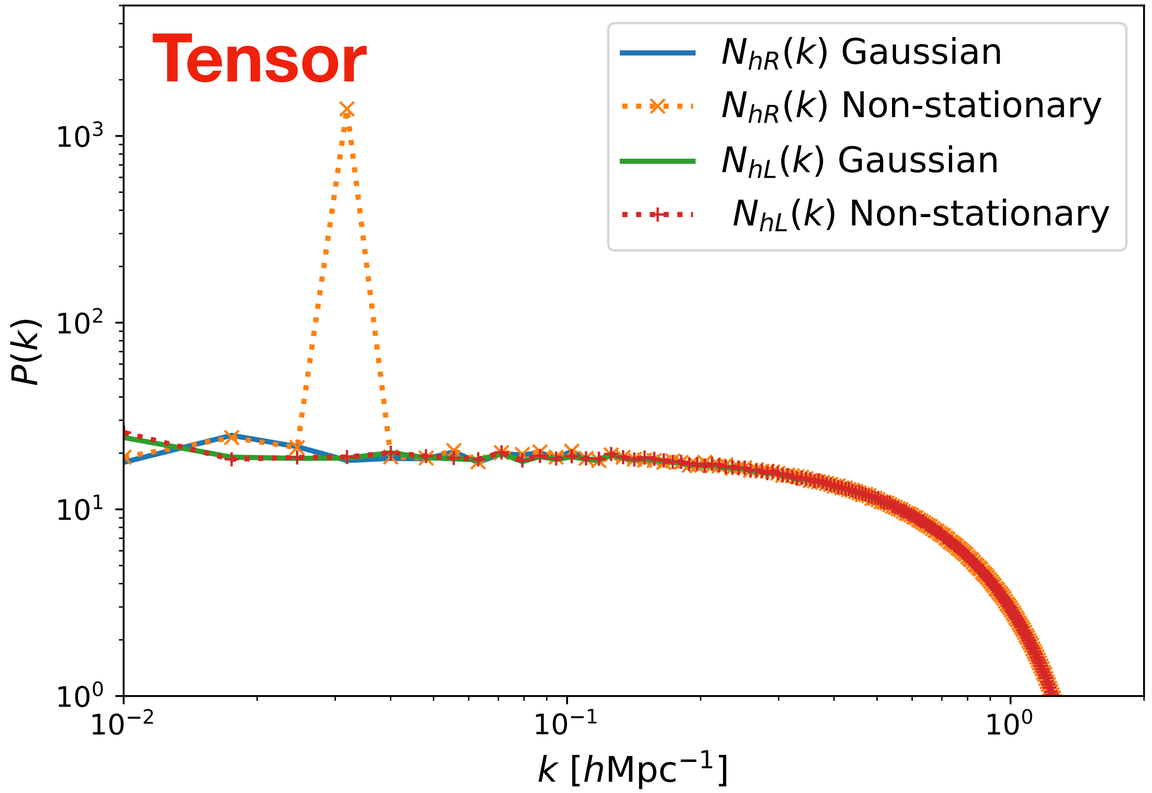

$$t_{ij} = \begin{pmatrix} \epsilon_0 + \epsilon_1 - \epsilon_z & \epsilon_2 & \epsilon_x \\ \epsilon_2 & \epsilon_0 - \epsilon_1 - \epsilon_z & \epsilon_y \\ \epsilon_x & \epsilon_y & \epsilon_0 + 2\epsilon_z \end{pmatrix}$$

$$v_a(\boldsymbol{K}) = v_R(\boldsymbol{K}) e_a^R(\hat{\boldsymbol{K}}) + v_L(\boldsymbol{K}) e_a^L(\hat{\boldsymbol{K}})$$

$$h_{ab}(\boldsymbol{K}) = h_R(\boldsymbol{K}) e_{ab}^R(\hat{\boldsymbol{K}}) + h_L(\boldsymbol{K}) e_{ab}^L(\hat{\boldsymbol{K}})$$

Zhu *and Pen, in prep, 2024*

Helical gravity waves: Nonlinearities

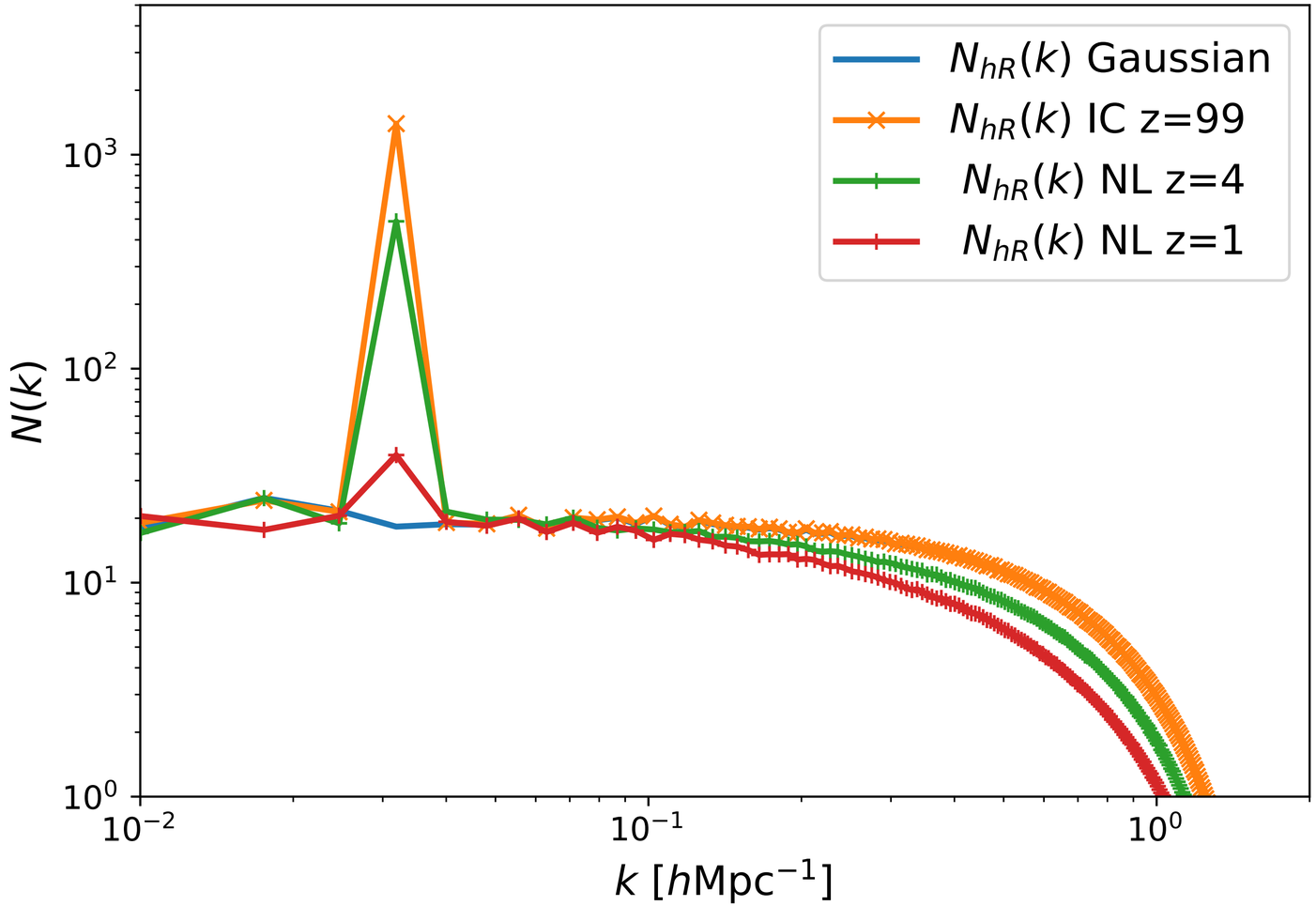

***Zhu** and Pen, in prep, 2024*

Example: BOSS NGC zbin1

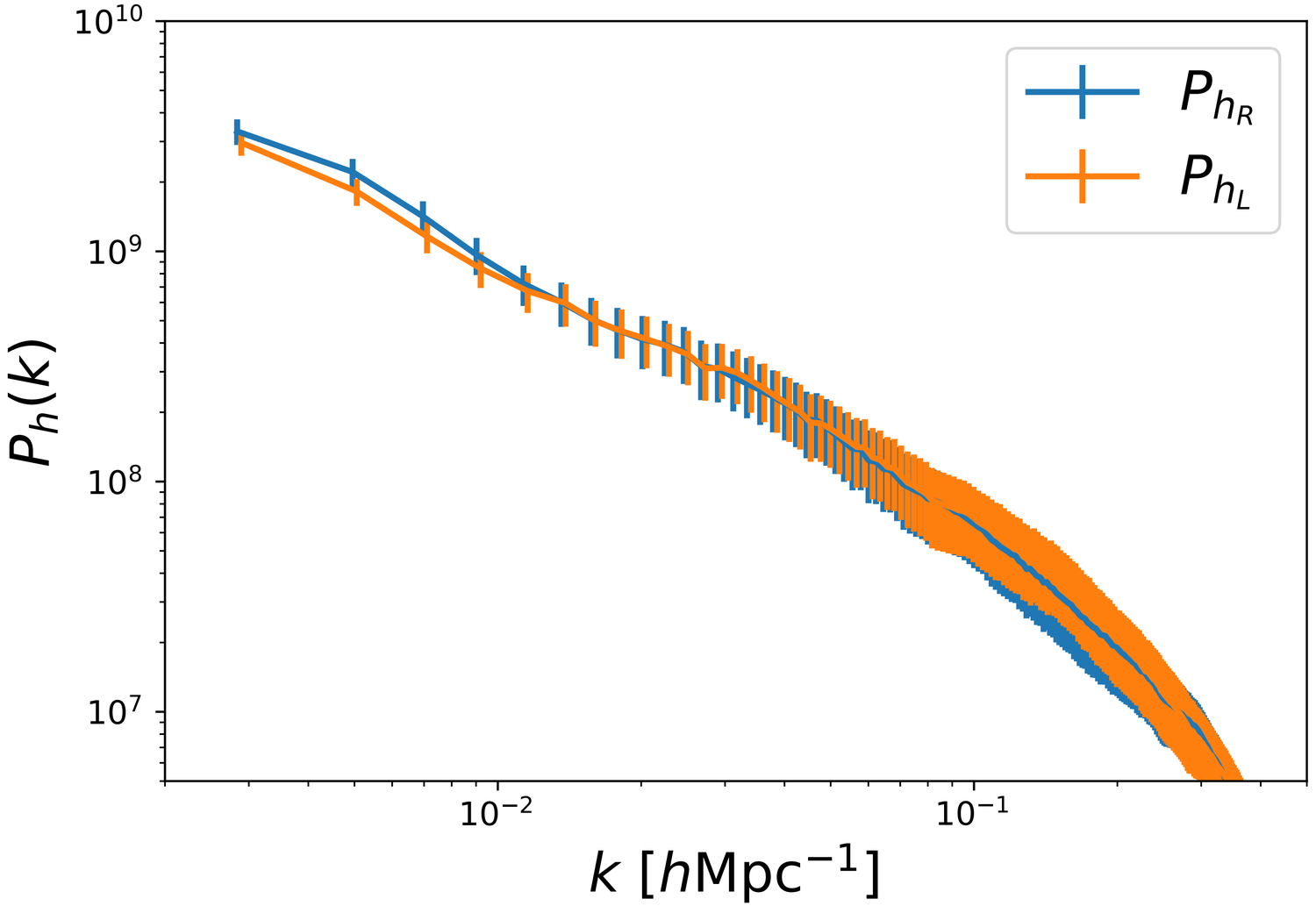

Zhu, *Pen, and Zang in prep, 2024*

Conclusion

- Low k radial modes lost due to 21 cm foregrounds
- No xcc with lensing, ISW, photo-z, …
- Measurements best at high k measurements
- Tidal reconstruction recovers large-scale information and xcc
- Probing new physics from parity violation

Thank you!

Symmetry breaking

- Parity violation in EW interactions (TD Lee and CN Yang, 1957 Nobel)

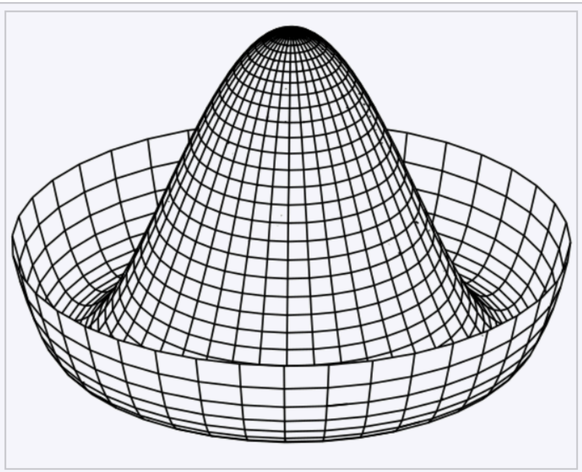

Graph of Goldstone's "sombrero" potential function $V(\phi)$.

Spontaneous symmetry breaking

Image from Wiki

Sea snails

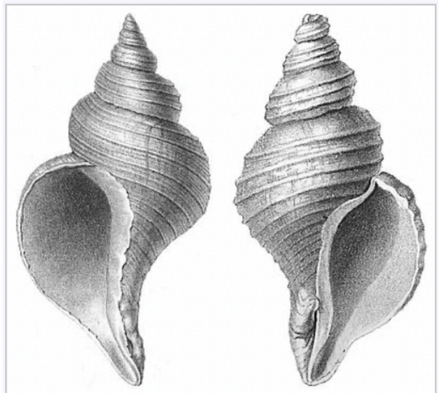

Shells of two different species of sea snail: on the left is the normally sinistral (left-handed) shell of *Neptunea angulata*, on the right is the normally dextral (right-handed) shell of *Neptunea despecta*

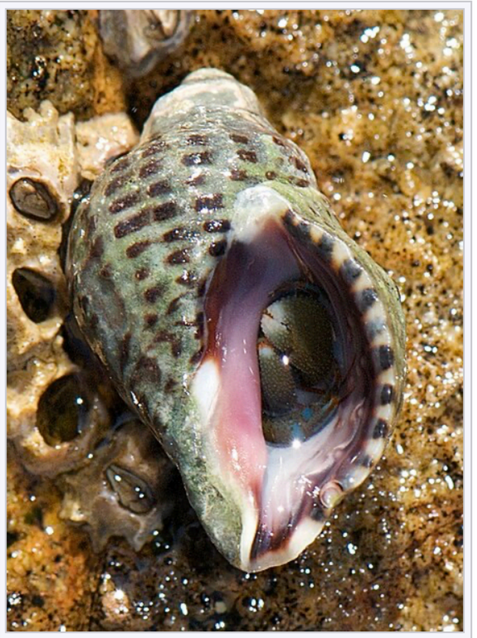

A hermit crab occupying a shell of *Acanthina punctulata* has been disturbed, and has retracted into the shell, using its claws to bar the entrance in the same way the snail used its operculum.

A closet

Helicity

- Macroscopic physics (gravity, E-M, etc) are parity symmetric
- any observed parity asymmetry direct window to initial conditions
- recent reports of detection (Hou+22, Philcox 22), upper bounds (Motloch+22)
- Large, abstract space of parity odd configurations in 4PCF, difficult to quantify covariances and look-elsewhere effect
- quadric estimator classification (Zhu and Pen in prep, 2024)

New method: Tidal reconstruction

- Local anisotropic gravity forces: $t_{ij} = \Phi_{L,ij}$
- Decomposition:

$$t_{ij} = \begin{pmatrix} \epsilon_0 + \epsilon_1 - \epsilon_z & \epsilon_2 & \epsilon_x \\ \epsilon_2 & \epsilon_0 - \epsilon_1 - \epsilon_z & \epsilon_y \\ \epsilon_x & \epsilon_y & \epsilon_0 + 2\epsilon_z \end{pmatrix}$$

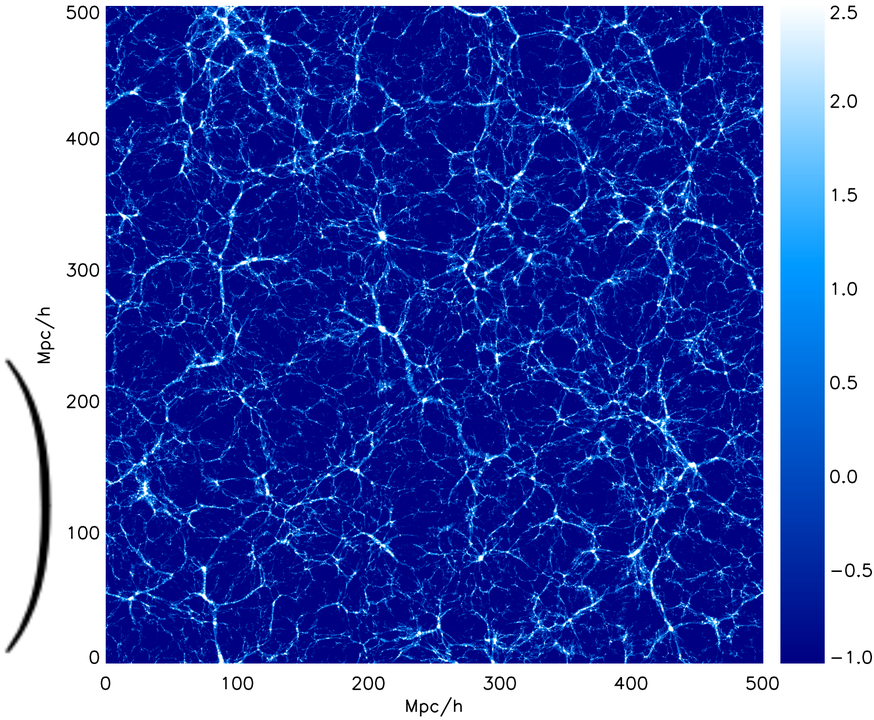

*Pen et al 2012; **Zhu** et al 2016, 2018, 2022; Zang, **Zhu*** et al 2024*

Tidal reconstruction: formalism

- Quadratic estimator:

$$\hat{\epsilon}_1(\boldsymbol{x}) = [\delta^{w_1}(\boldsymbol{x})\delta^{w_1}(\boldsymbol{x}) - \delta^{w_2}(\boldsymbol{x})\delta^{w_2}(\boldsymbol{x})]/2,$$
$$\hat{\epsilon}_2(\boldsymbol{x}) = \delta^{w_1}(\boldsymbol{x})\delta^{w_2}(\boldsymbol{x}),$$
$$\hat{\epsilon}_x(\boldsymbol{x}) = \delta^{w_1}(\boldsymbol{x})\delta^{w_3}(\boldsymbol{x}),$$
$$\hat{\epsilon}_y(\boldsymbol{x}) = \delta^{w_2}(\boldsymbol{x})\delta^{w_3}(\boldsymbol{x}),$$
$$\hat{\epsilon}_z(\boldsymbol{x}) = [2\delta^{w_3}(\boldsymbol{x})\delta^{w_3}(\boldsymbol{x}) - \delta^{w_1}(\boldsymbol{x})\delta^{w_1}(\boldsymbol{x}) - \delta^{w_2}(\boldsymbol{x})\delta^{w_2}(\boldsymbol{x})]/6,$$

where

$$\delta^{w_j}(\boldsymbol{k}) = i\hat{k}_j w(k)\delta(\boldsymbol{k})N_{\epsilon_\alpha}^{1/2},$$

Pen et al 2012; Zhu et al 2015, 2022